Extension of MST/SCRF Method to Organic Solvents: *Ab Initio* and Semiempirical Parametrization for Neutral Solutes in CCl$_4$

F. J. LUQUE* and M. BACHS

Departament de Farmàcia. Unitat Fisicoquímica, Facultat de Farmàcia, Universitat de Barcelona, Avgda. Diagonal s/n, Barcelona 08028, Spain

C. ALEMÁN

Departament d'Enginyeria Química, ETSEIB, Universitat Politècnica de Catalunya, Avgda. Diagonal 647, Barcelona 08028, Spain

MODESTO OROZCO*

Departament de Bioquímica, Facultat de Química, Universitat de Barcelona, Martí i Franquès 1, Barcelona 08028, Spain

ABSTRACT

The self-consistent reaction field (SCRF) method proposed by Miertus, Scrocco, and Tomasi (MST) was extended to solutions of neutral solutes in CCl$_4$. A detailed parametrization of the solute/solvent interface and of the "hardness" atomic parameters determining the van der Waals interactions was performed from comparison with experimental data and Monte Carlo simulations. The parametrization was carried out at both *ab initio* (6-31G*) and semiempirical (MNDO, AM1, PM3) levels. The MST/SCRF optimized versions provide accurate estimates of the free energy of solvation in CCl$_4$ for the series of molecules studied. Furthermore, a precise description of the solvent effect on different chemical processes in CCl$_4$ solution supports the reliability of the parametrization. © 1996 by John Wiley & Sons, Inc.

* Correspondence may be addressed to either author.

Introduction

The solvent plays a key role in the thermodynamics and kinetics of chemical systems.[1] An understanding of any chemical process in solution cannot be achieved without an accurate description of the solvent effect, which must be explicitly incorporated in theoretical simulations. Unfortunately, the large number of solvent molecules needed to mimic a dilute solution makes such description difficult. The high cost of the quantum mechanical (QM) methods limits their usefulness to the study of specific interactions within the supermolecule approach. It has been necessary to develop alternative strategies, which can broadly be classified in three categories: classical models, hybrid QM-classical methods, and self-consistent reaction field (SCRF) algorithms. Classical and hybrid QM-classical methods use a discrete representation of the solvent molecules, but differ in the treatment of the solute, which is described as a classical or QM entity, respectively. SCRF methods treat the solute at the QM level, while the solvent is represented as a dielectric continuum.

Since the seminal works of Onsager[2] and Kirkwood and Westheimer,[3] a large number of SCRF methods have been developed.[4] All of them lay special emphasis on the determination of the electrostatic contribution to the free energy of solvation, ΔG_{solv}, which is evaluated assuming that the infinite dielectric medium, the solvent, reacts against the solute charge distribution generating a reaction field, which in turn interacts with the solute. The main differences between the SCRF methods lie in the shape of the solute/solvent interface and in the definition of the reaction field. The use of realistic cavities and a precise treatment of the solvent reaction field are crucial factors in determining the reliability of the SCRF results.

In the early 1980s Miertus, Scrocco, and Tomasi[4c] (MST) developed an accurate method to compute the electrostatic component of ΔG_{solv}. The reaction field is rigorously defined in terms of the molecular electrostatic potential (see below), avoiding the use of truncated expansions, and cavities adapted to the molecule are considered (see ref. 5 for details). Extension of the method to nonelectrostatic contributions to ΔG_{solv} is straightforward,[6] and its implementation in different QM frameworks is not difficult.[7] An *ab initio* QM(6-31G*)-optimized version has recently been reported,[8] which estimates

free energies of hydration, ΔG_{hyd}, for a large series of molecules with a root mean square deviation (rms) of 0.75 kcal/mol from experimental data. Indeed, semiempirical versions[9] also provide good results (rms around 1 kcal/mol). The development of these versions involved a very limited parametrization and most of the optimized parameters were transferable. Other SCRF methods have also proved to be very powerful in the study of chemical systems in aqueous solution.[10]

Despite the large number of SCRF methods developed to simulate aqueous solutions, not much attention has been paid to the thermodynamic properties of solvation, particularly the free energy of solvation, in nonaqueous media. To our knowledge, besides some studies developed by Tomasi's group,[11] there is to our knowledge only one systematic SCRF study of solvation in an apolar medium (*n*-hexadecane), recently reported by Giesen et al.,[12] which states the suitability of SCRF methods to represent nonpolar solvents.

In this article the parametrization of the MST method to deal with calculations of free energies of solvation for neutral solutes in CCl_4 is presented. The MST method has been parametrized at the *ab initio* 6-31G*,[13] AM1,[14] MNDO,[15] and PM3[16] wave functions. Experimental data, as well as information gained from Monte Carlo simulations, were used in the parametrization. To examine the reliability of the final set of parameters, test calculations were performed to verify the ability of the optimized MST method to describe different chemical processes in CCl_4.

Methods

The underlying assumption shared by SCRF methods is the partitioning of the solute transfer from the gas phase into solution in several steps: the solute cavity is built up inside the solvent, a van der Waals (VW) entity is generated within the cavity, and the entity is charged up until the charge distribution of the solute in solution is reached. If changes in the internal degrees of freedom of the solute induced upon solvation are neglected, the total free energy of solvation, ΔG_{solv}, can then be expressed as

$$\Delta G_{solv} = \Delta G_{cav} + \Delta G_{vw} + \Delta G_{ele} \qquad (1)$$

In eq. (1) ΔG_{cav}, ΔG_{vw}, and ΔG_{ele} are the reversible works to build up the cavity, to generate the van der Waals entity, and to charge up the

solute inside the solvent, respectively. Within this framework, the ΔG_{vw} term, when it is parameterized from experimental data, also includes contributions derived from volume effects. A common reference state is assumed in both the gas phase and solution.

In the MST method the electrostatic component, ΔG_{ele}, is determined from the linear free energy response (LFER) theory[17] according to eq. (2), where the Hamiltonian in solution, $\hat{H}$, stems from the addition of the reaction field operator, $\hat{V}_R$, to the gas phase Hamiltonian, $\hat{H}^o$ [eq. (3)]. The perturbation operator is computed from the surface charge distribution, $\sigma(s)$, induced in the solute/solvent interface by the solute charge distribution.

$$\Delta G_{ele} = \langle \psi | \hat{H} | \psi \rangle - \langle \psi^0 | \hat{H}^0 | \psi^0 \rangle$$
$$- 1/2\left(\langle \psi | \hat{V} | \psi \rangle + \int \rho_{nuc} V_\sigma(s)\, ds \right) \quad (2)$$

$$\left(\hat{H}^0 + \hat{V}_R \right) \Psi = E\Psi \quad (3)$$

$$\hat{V}_R = \int_S \frac{\sigma(s)}{|r_0 - r|} dS. \quad (4)$$

Eq. (4) can be simplified if the cavity surface is divided into M elements S_i small enough to consider the charge distribution $\sigma(s)$ constant inside them [see eq. (5)].

$$\hat{V}_R = \sum_{i=1}^{M} \frac{\sigma(s_i)S_i}{|r_0 - r|} = \sum_{i=1}^{M} \frac{q_i}{|r_0 - r|}. \quad (5)$$

By solving the Laplace equation with the appropriate boundary conditions, the charge density at each surface element, $\sigma(s_i)$, is determined according to eq. (6), where the total electrostatic potential, V_T, includes both solute and solvent contributions. The iterative nature of the method clearly stems from the mutual dependence between the reaction field operator and the solute wave function [eqs. (3)–(6)].

$$\sigma(s_i) = -\frac{\varepsilon - 1}{4\pi\varepsilon}\left(\frac{\partial V_T}{\partial n} \right) \quad (6)$$

where ε is the dielectric constant of the solvent and n the unitary vector normal to the surface.

The electrostatic potential of the solute, which is rigorously determined as the expectation value of the r^{-1} operator,[18] was computed at the 6-31G* level within the *ab initio* framework, while the *ortho* method[19] was used at the semiempirical level.

The preference of the *ortho* approach over the *quasi-ab initio*[20] to compute semiempirical electrostatic potentials has been explained in detail elsewhere.[9, 19b]

Cavitation and van der Waals contributions, often referred to as "steric" components of ΔG_{solv}, are expected to be large in nonpolar solvents. They are usually determined from the nuclear configuration according to simple equations that include empirical parameters. Among the different expressions proposed to evaluate the cavitation term, Pierotti's scaled particle theory, adapted to nonspherical shapes, was used.[21a] This formulation works fairly well for solvents of small size, even when they are polar, protic, or hydrogen bonded[5e]; and results presented here confirm the goodness of the approach (see below). There are different formalisms to evaluate the van der Waals term.[6, 22] In a previous study,[8a] we found that a simple relationship with the molecular surface [eq. (7)] can capture such a contribution upon fitting of the van der Waals parameters (ξ_i) to experimental data. The atomic surfaces (S_i) were computed using GEPOL[5b, c] from the scaling of atomic van der Waals radii [C, 1.5 Å; N, 1.5 Å; O, 1.4 Å; H, 1.2 Å; H (bound to polar atoms), 0.9 Å[8a, †]]. This procedure permits the incorporation of other contributions not explicitly considered in the model. However, in this study the inclusion of an optimized independent term in eq. (7) and the addition of molecular volume effects[23] were also examined, but no improvement was achieved in the fitting.

$$\Delta G_{vw} = \sum_i \xi_i S_i. \quad (7)$$

The parameters involved in the evaluation of ΔG_{solv} must be modified when the SCRF method parametrized for aqueous solution is extended to other solvents. Thus, the change in the dielectric constant reflects the different polarization response of the solvent to the solute charge distribution (a value of 2.228 for CCl_4 at 298 K was used[24]). The cavity size, which should be related to the first peak in the solute–solvent radial distribution function (RDF), varies with the intensity of the forces between solute and solvent molecules. Indeed, the change of the cavitation parameters accounts for the intrinsic ability of the solvent to modify its internal structure to accommodate the solute (parameters for CCl_4 were taken from the data

---

† The van der Waals radius for H bound to heteroatoms used in semiempirical calculations was 0.8 (see ref. 9).

compiled by Pierotti[21a]). Finally, the van der Waals parameters should be modified to capture changes in dispersion–repulsion interactions, as well as contributions related to the different size of solvent molecules.

The parametrization was performed at the *ab initio* 6-31G* and semiempirical AM1, MNDO, and PM3 levels, which provided good estimates of ΔG_{hyd} for a series of prototypical molecules.[8, 9] Values of ΔG_{solv} in CCl_4 were obtained from experimental CCl_4/water partition coefficients[25a] according to eq. (8). Experimental values of ΔG_{hyd} were used in eq. (8).[25b–d] For the series of molecules studied, the geometry was optimized in the gas phase at the corresponding calculational level and then kept frozen in solution. The neglect of geometry relaxation was not expected to introduce large errors. Furthermore, this residual effect was captured, at least partly, in the parametrization, as stated by previous results in aqueous solutions.[8, 9, 26]

$$\Delta G_{solv}^{CCl_4} = \Delta G_{hyd} - 2.303RT \log P. \qquad (8)$$

Monte Carlo (MC) simulations were performed to help us determine the best solute/solvent interface. These simulations were carried out with a twofold purpose. First, the solute–CCl_4 RDFs were determined to examine the distribution of the solvent molecules around the solute, and to estimate the average distance from the solute to solvent molecules. The RDFs were obtained for five molecules (water, ammonia, ethanol, ethylamine, and acetone) using two different sets of charges for the solute (see below).

With the aim to determine the solute/solvent interface (i.e., to define the size of the solute cavity), Monte Carlo–Free Energy Perturbation (MC–FEP) simulations were also performed to estimate the magnitude of the different contributions to the free energy of solvation. The electrostatic term was determined from the work necessary to annihilate the solute charge. In this case MC–FEP simulations were performed using two different sets of charges for the solute (see below). The steric term was determined from the work needed to annihilate the van der Waals parameters of the molecule, once the charges were already annihilated. These simulations were performed for ethanol, ethylamine, acetone, acetic acid, and pyridine.

MC simulations were carried out using BOSS 3.4 (ref. 27) at the NPT ensemble (1 atm; 298 K) using preferential sampling and periodic boundary

conditions. A single solute was immersed in a 21025 $\mathring{A}^3$ pre-equilibrated cubic box containing 128 CCl_4 molecules. Standard Optimized Parameters for Liquid Simulations (OPLS)[28] parameters for electrostatic and van der Waals interactions were used for the solutes. In addition, 6-31G* (ESP) atomic charges[29] were also used with standard OPLS Lennard–Jones parameters to evaluate the electrostatic term in MC–FEP simulations. RDFs were determined from averaging over 3 million configurations, after an equilibration of 2 million configurations. MC–FEP simulations were performed in 11–21 windows using the double-wide sampling technique. For each window the system was equilibrated at least over 2 million configurations and the average was done for 2–3 million configurations. During the annihilation of the van der Waals parameters the bond lengths were reduced to 0.2 $\mathring{A}$ to increase the efficiency of the sampling. In all cases the hysteresis and the standard deviations were small, which gives confidence to the protocol of the simulation.

Finally, solvent-induced solvatochromic shifts were calculated to test qualitatively the reliability of the solute/solvent interface. They were carried out at the semiempirical level according to the detailed treatment of nonequilibrium processes reported by Aguilar et al.,[30] in which special attention is paid to the boundary conditions. A small 2 × 2 configuration interaction (CI) was used to avoid the overestimation of correlation effects within semiempirical methods.

Ab initio gas phase and SCRF calculations were performed using Gaussian 92 (ref. 31) and a modified version of MonsterGauss,[32] respectively. Semiempirical calculations were carried out using a modified version of MOPAC-93, Rev. A,[33] which includes the routines for MST calculations. All the calculations were performed on a Cray Y-MP computer and on Hewlett–Packard and Sun workstations in our laboratory.

Results and Discussion

SCRF results for aqueous solution are highly dependent on the size of the cavity that defines the boundaries of the solute.[7c, 8] Such dependence for nonpolar solvents is expected to be reduced, but it may still be large, because the cavity size modulates the magnitude of the different free energy contributions. Accordingly, the determination of the cavity size is a delicate step in the parametriza-

tion of the MST method, even more when the magnitude of the different contributions are not directly measurable.

SELECTION OF CAVITY

The determination of the solute/solvent interface in an apolar solvent is less clear than in aqueous solution. However, it can be assumed that the reaction field induced by the solute charge distribution mainly arises from those CCl_4 molecules placed in the first solvation layer. Therefore, it can be argued that the solute/solvent interface should be related to the first peak in the solute–CCl_4 RDF. In particular, a reasonable choice is to define the solute boundaries in terms of the distance from the solute to the first atom of the solvent, typically a chlorine atom.

MC simulations for water, ammonia, ethanol, ethylamine, and acetone showed RDFs with broad peaks located at 4.2–5.2 Å from the solute (Fig. 1). It is worth noting the close similarity exhibited by RDFs determined from either OPLS ($q_C = 0.248$ e$^-$) or ESP ($q_C = 0.420$ e$^-$) charges, which supports the reliability of the RDFs. For comparison, additional simulations (data not shown) were performed neglecting Coulombic interactions for the

CCl_4 molecules. In this case, a loss of solvent structure around the solute was found, which stresses the relevance of solute–solvent and solvent–solvent electrostatic interactions. Taking into account the RDFs, the C—Cl bond length and the van der Waals radii of N and O, the solute/solvent boundary can be estimated to be placed at 1.6–2.2 times the atomic van der Waals radii. SCRF test calculations revealed that the use of a factor larger than 2.0 led to a small but significant loss in the accuracy of the free energies of solvation when compared with the experimental data.

Owing to the lack of direct thermodynamic data available for comparison, the use of the RDFs to locate the solute/solvent interface is a reasonable choice. However, it could also be assumed that the solute/solvent interface is mainly determined only by the solute structure, and consequently a cavity similar to that used in aqueous solution, which should be transferable to different solvents, can be defined. In this context, a systematic 6-31G* SCRF study was performed changing the factor (κ) that scales the van der Waal radii between 1.7 and 2.0 and also between 1.3 and 1.4 (the choice of κ = 1.25, which was used to define the solute cavity in aqueous solution, provided worse results). For each scaling factor the electrostatic and cavitation terms
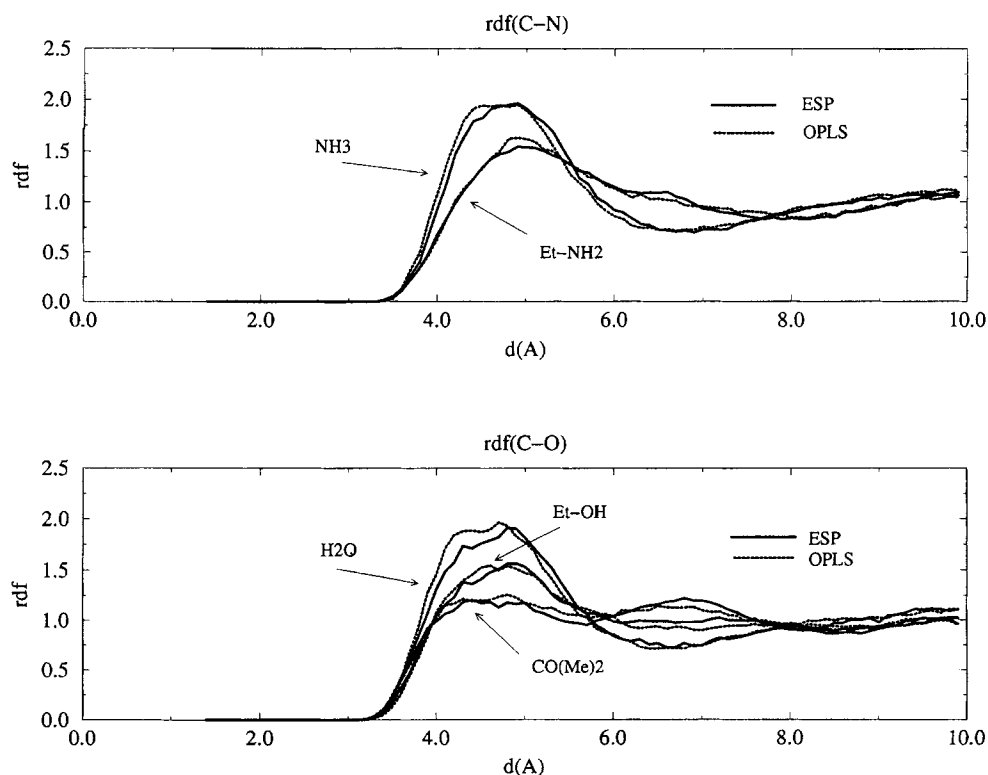

FIGURE 1. Radial distribution functions for several solutes in CCl_4 solution.

were evaluated and the van der Waals parameters were optimized from the fitting to the experimental free energies of solvation [eq. (9)].

$$\Delta G_{residual} = \Delta G_{sol}^{exp} - \Delta G_{cav} - \Delta G_{ele}. \qquad (9)$$

The best agreement between experimental and calculated ΔG_{solv} was found for a scaling factor of 1.8, which provides an rms deviation of 0.4 kcal/mol. Nevertheless, the dependence of the results on the solute cavity was small. For comparison, the use of a small cavity ($\kappa = 1.4$) provides an rms deviation of only 0.55 kcal/mol. This small dependence can clearly be attributed to the lower strength of electrostatic interactions in an apolar solvent like CCl_4 in comparison with aqueous solution.

The small dependence of ΔG_{solv} on the cavity size has two important consequences for the optimization of the MST model: if the van der Waals term is properly fitted, even an incorrect cavity can provide accurate estimates of ΔG_{solv}; the agreement between experimental and theoretical ΔG_{solv} should not be the only guideline to select the proper cavity size. The first point clearly favors our purposes, since ΔG_{solv} is the most important property to be determined from these simulations. However, an improper cavity will not only unbalance the relative weights of the different contributions to ΔG_{solv}, but will also incorrectly estimate the solvent polarization effect on the solute wave function.

To examine the proper selection of the cavity, MC–FEP simulations were performed to estimate the magnitude of the electrostatic and steric terms to ΔG_{solv} (see Methods). These simulations allow us to have an independent test about the size of the cavity, which greatly modulates the contribution of the different terms, particularly of the electrostatic one. This term can be estimated from the annihilation of the solute charges in a box of CCl_4 solvent molecules. Both OPLS (solute and solvent) and ESP (solute)/OPLS (solvent) charges were considered in the simulations. The values of ΔG_{ele} determined with the two sets of charges lie in the range of a few tenths kcal/mol and, in fact, were never lower than -0.2 kcal/mol. Certainly, MC–FEP values are not accurate estimates of ΔG_{ele}, mainly due to the neglect of polarization effects in classical FEP simulations and to the possible mixing between electrostatics and dispersion effects in the force field. These two effects should underestimate the magnitude of ΔG_{ele} in MC–FEP calculations. However, it is difficult to conceive that these

effects may account for the discrepancy (greater than one order of magnitude) found with regard to the SCRF results derived using a scaling factor of 1.3–1.4. In fact, choice of a cavity similar to that used for aqueous solution provides values of ΔG_{ele} around -2.5 kcal/mol, on average, for the 27 molecules studied; and for some molecules like p-hydroxybenzaldehyde, the electrostatic term is lower than -5 kcal/mol. Much more reliable estimates of ΔG_{ele} are obtained for $\kappa \approx 1.8$.

Further support for the enlargement of the cavity with respect to that used in aqueous solution comes from the evaluation of the steric contribution to ΔG_{solv}. This contribution can be approximately determined using MC–FEP simulations from the annihilation of the van der Waals parameters, once the charges have been previously annihilated. The magnitude of the MC–FEP steric contribution can be compared with the SCRF value, which was determined from the difference between the free energy of solvation and the electrostatic term [eq. (1)]. This difference should depend on the cavity size, since ΔG_{ele} increases (in absolute value) as the cavity is reduced, and accordingly these calculations provide an additional test about the goodness of the cavity. Note that the determination of the steric contribution is computed without any assumption at the MC–FEP level.

The MC–FEP values of the steric contribution are given in Table I, which also displays the SCRF values determined for two different scaling factors: $\kappa = 1.8$ and 1.25 (this was the scaling factor used to build up the cavity in the 6-31G* version of the MST model for aqueous solution[8a]). To compute the SCRF steric term [see eq. (1)], the

TABLE I.
Contribution (kcal / mol) of Steric Term to Free Energy of Solvation Determined from MC – FEP Simulations and SCRF Calculations.

Molecule	MC –FEP	SCRF ($\kappa = 1.8$)	SCRF ($\kappa = 1.25$)
Ethanol	−1.9	−2.4	−0.3
Ethylamine	−1.8	−2.3	0.0
Acetone	−3.0	−2.5	−0.4
Acetic acid	−1.4	−2.4	0.8
Pyridine	−4.4	−4.3	−2.5

The SCRF values were determined at two different cavities defined by the scaling factors $\kappa = 1.8$ and 1.25. The SCRF steric term was estimated from the difference between the experimental ΔG_{solv} and the 6-31G* SCRF ΔG_{ele} (see text for details).

ΔG_{ele} evaluated at the SCRF 6-31G* level was substracted to the experimental values of ΔG_{solv} (obviously very similar results to those reported in Table I for the SCRF steric term were found upon addition of the cavitation and van der Waals terms, after fitting the van der Waals parameters for each scaling factor). Inspection of the results shows the agreement between the MC–FEP values and the SCRF estimates determined at $\kappa = 1.8$. Furthermore, the SCRF values for $\kappa = 1.25$ are clearly underestimated, and in some cases the opposite sign is obtained. This is clearly stated by the rms, error, which amounts to 2.0 kcal/mol for the cavity defined in aqueous solution; for the largest cavity ($\kappa = 1.8$) it is only 0.6 kcal/mol. Certainly, the good agreement found for this latter cavity may be somewhat fortuitous; but it is completely clear that the large cavity performs well, and the water-adapted cavity is too small to represent properly the solute/solvent interface in CCl_4 solutions.

Additional support to the enlargement of the cavity also comes from the polarization of the solute charge distribution, which is greatly influenced by the cavity size. This effect is expected to be small, but significant, as stated from a simple inspection of Onsager's equation.[2] Too small a cavity will overestimate the polarization, leading to an artefactual increase in the solvent-induced dipole moment. MST calculations performed with $\kappa \approx 1.3–1.4$ increased the gas phase dipole moment by around 12%. This finding contrasts with the very small effect found by Gao from MC-QM(AM1)/MM calculations.[34] These latter mixed calculations can be criticized for the use of a non-polarizable force field for CCl_4, but again it is difficult to attribute the large discrepancy to this source of error alone. In this respect, larger cavities, like that defined by $\kappa = 1.8$, reduce the magnitude of the solvent-induced dipole to a half (the induced dipoles were not significantly reduced by further increase in the cavity, within reasonable limits). This effect is still larger than that found from MC-QM/MM calculations, but it fits much better.

Finally, qualitative evidence comes from the solvent-induced solvatochromic shifts in the electronic spectra of acetone.[35] At this point, it should be emphasized that our purpose is not to reproduce the well-known red shift observed in CCl_4, because it is expected to be modulated by the dispersion interactions involved in excited and ground states, which are not properly dealt with in the MST model, and are also due to the small CI

used to compute the excitation energy.[36] However, empirical estimates of the dispersion contribution available from the literature[36d] may be used to provide an approximate estimate of the solvent-induced shift.

Results in Table II, which gives the solvent-induced shifts for the vertical transitions $S_0 \rightarrow T_1$ and $S_0 \rightarrow S_1$, show the ability of the MST model to reproduce the blue shift for acetone in aqueous solution. The agreement, which was not completely unexpected according to previous studies,[30, 36b, c, 37] gives qualitative confidence to the results for CCl_4. In this respect, a red shift is obtained after addition of the dispersion correction when the scaling factor cavity $\kappa = 1.8$ is used; less reasonable results are found when a smaller cavity ($\kappa = 1.2$) is used (the factor of 1.2 was used to define the cavity in the semiempirical MST model for aqueous solution[9]).

In summary, the whole of these tests suggest that within the framework of the MST model, a large cavity, probably defined from the scaling of van der Waals radii by a factor around 1.8, may provide a suitable representation for the solute embedded in a CCl_4 solution. Nevertheless, it must be stressed that this is an *empirical* selection of the cavity for the MST model, largely motivated by the lack of direct thermodynamic data for the different energetic contributions. Indeed, these tests do not preclude the use of smaller cavities in other SCRF models, which may provide accurate estimates of ΔG_{solv} after a careful parametrization. Finally, even though the same cavity definition was adopted for every contribution to the ΔG_{solv} in this study, the use of different cavities for evaluating the different terms can be envisaged as an alternative parametrization procedure.

TABLE II.
Solvent Shift (kcal / mol) of Acetone.

Solvent	Method	$S_0 \rightarrow T_1$	$S_0 \rightarrow S_1$
H_2O^a (exptl. +4.5)			
	AM1	+4.8	+4.5
	MNDO	+4.7	+4.3
	PM3	+5.0	+4.8
$CCl_4{}^a$ (exptl. −1.4)			
	AM1	−1.0, +1.4	−1.0, +1.5
	MNDO	−1.7, +0.9	−1.6, +1.0
	PM3	−1.5, +1.6	−1.5, +1.5

Values for CCl_4 solutions were determined using a scaling factor of $\kappa = 1.8$ (plain text) and $\kappa = 1.20$ (italics). See text for details.
[a] Ref. 35.

6-31G* PARAMETRIZATION

Values of ΔG_{solv} for the series of molecules and its components are shown in Table III, whereas the optimized van der Waals parameters are given in Table IV. All the contributions to ΔG_{solv} were determined using the cavity built up from the scaling factor $\kappa = 1.8$. Relevant differences are found when these results are compared with values for aqueous solution. Thus, the electrostatic

contribution is the leading term in the aqueous solution, but it accounts for only 17% of ΔG_{solv} in CCl_4. In addition the steric term is always negative, in contrast with results for the aqueous solution, where it has a net positive value. The ultimate reason for these differences lies in the intrinsic electronic structure of water and CCl_4 molecules. Thus, the bigger size and less polarizable nature of CCl_4 makes this solvent less structured than bulk water. Therefore, the generation of

TABLE III.
Ab Initio 6-31G* SCRF and Experimental Free Energies of Solvation (kcal / mol) in CCl_4.

Molecule	ΔG_{ele}	ΔG_{cav}	ΔG_{vw}	ΔG_{SCRF}	ΔG_{exp}
Phenol	−0.9	13.4	−18.4	−5.9	−6.1
Methanol	−0.8	8.6	−10.4	−2.6	−2.2
Acetic acid	−1.0	10.6	−13.7	−4.2	−3.4
Methyl acetate	−0.8	12.6	−16.3	−4.5	−3.7
Pyridine	−0.7	12.6	−17.0	−5.0	−5.0
Acetone	−1.0	11.7	−14.9	−4.2	−3.5
Ethanol	−0.7	10.4	−12.8	−3.0	−3.1
n-Propanol	−0.7	12.1	−15.0	−3.6	−3.7
n-Butanol	−0.7	13.7	−17.2	−4.2	−4.2
n-Pentanol	−0.7	15.3	−19.5	−4.8	−5.0
n-Hexanol	−0.7	16.9	−21.6	−5.4	−5.7
n-Heptanol	−0.7	18.5	−23.9	−6.1	−6.5
Propionic acid	−1.0	12.3	−16.0	−4.6	−4.3
Butyric acid	−1.0	13.8	−18.0	−5.1	−5.0
Ethylacetate	−0.8	14.3	−18.6	−5.0	−4.4
p-Hydroxybenzaldehyde	−1.6	15.1	−21.5	−7.9	−8.2
p-Nitrophenol	−1.8	15.5	−22.1	−8.5	−9.4
m-Nitrophenol	−1.8	15.5	−22.1	−8.4	−8.8
p-Methylphenol	−0.9	15.1	−20.7	−6.5	−6.1
o-Methylphenol	−0.8	14.8	−20.3	−6.2	−6.8
Acetophenone	−0.9	15.9	−22.0	−7.1	−6.4
Aniline	−0.8	13.7	−18.8	−5.9	−5.7
Ethylamine	−0.5	10.8	−13.3	−3.0	−2.8
n-Propylamine	−0.5	12.5	−15.5	−3.6	−3.6
n-Butylamine	−0.5	14.0	−17.7	−4.2	−4.2
Trimethylamine	−0.2	12.4	−15.3	−3.1	−3.1
Diethylamine	−0.2	14.3	−17.8	−3.7	−4.1

The SCRF free energy is decomposed into electrostatic (ΔG_{ele}), cavitation (ΔG_{cav}), and van der Waals (ΔG_{vw}) terms.

TABLE IV.
Ab Initio 6-31G* and Semiempirical (AM1, MNDO, PM3) van der Waals Parameters Optimized for MST–SCRF Calculations in CCl_4 (kcal / mol Å²).

Atom	ξ (6-31G*)	ξ (AM1)	ξ (MNDO)	ξ (PM3)
C	−0.1080	−0.1077	−0.1086	−0.1084
N	−0.0901	−0.0902	−0.0912	−0.0909
O	−0.0929	−0.0954	−0.0939	−0.0936
H (carbon)	−0.0771	−0.0783	−0.0786	−0.0786
H (heteroatom)	−0.0771	−0.0783	−0.0786	−0.0786

a cavity is less difficult than in a highly polar solvent like water. Furthermore, from the larger cavity in CCl_4 than in water and the magnitude of the corresponding atomic van der Waals parameters (Table IV), more favorable van der Waals interactions are expected in CCl_4 than in aqueous solution.

Comparison between MST/6-31G* and experimental ΔG_{solv} in CCl_4 demonstrates the quality of the model (Fig. 2). Thus, the average error and the ratio $\Delta G_{exp}/\Delta G_{SCRF}$ are close to the optimum values, indicating the lack of systematic errors. The rms deviation indicates a random error of only 0.4 kcal/mol, which is 0.35 kcal/mol smaller than that found for the MST/6-31G* ΔG_{hyd}.[8a,9b] Finally, the regression ($r = 0.97$) explains more than 94% of the experimental data, which together shows excellent agreement between experimental and theoretical ΔG_{solv}.

The solvent polarization on the solute charge distribution is illustrated from the change in dipole moments upon solvation (Fig. 3). A small but consistent increase (around 6%) in the dipole with respect to the gas phase values is found. Such an increase reflects the low but significant magnitude of the reaction field generated by the CCl_4 solvent. It should be noted that the existence of this reaction field is a requisite of the theory of polarizable fluids for all solvents with $\varepsilon > 1$.[17] It is also worth noting that the magnitude of the induced dipole is relatively insensitive to moderate changes in the cavity size.
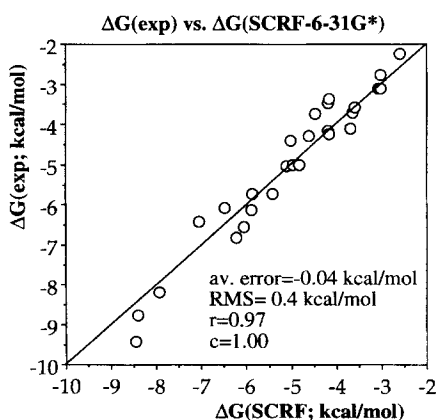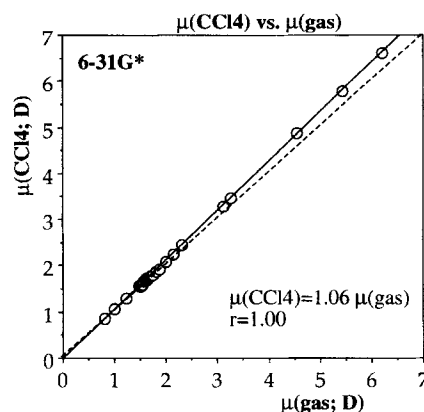

FIGURE 3. Comparison between 6-31G* dipoles in gas phase and in CCl_4 solution. The dashed line corresponds to the ideal regression equation.

SEMIEMPIRICAL PARAMETRIZATION

The parametrization followed a similar procedure than that reported at the *ab initio* level. Nevertheless, the cavity was not changed, and the optimum *ab initio* scaling factor ($\kappa = 1.8$) was used. The optimized van der Waals parameters are shown in Table IV, and the final ΔG_{solv} values are given in Table V.

Semiempirical results are very similar to the *ab initio* values, as noted in the correlation (Fig. 4) between semiempirical and *ab initio* ΔG_{solv}. Furthermore, comparison of *ab initio* induced dipoles (Fig. 3) with the semiempirical ones (Fig. 5) demonstrates the ability of the semiempirical methods to reproduce the solvent-induced changes in CCl_4 solutions.

Comparison with experimental data allowed us to determine the quality of the optimized models. In all cases semiempirical estimates of ΔG_{solv} correlate very well ($r = 0.97$) with experimental data. The $\Delta G_{exp}/\Delta G_{SCRF}$ ratio (1.00 in all cases), the average deviations (0.03–0.04), and the rms deviations (0.45–0.50 kcal/mol) demonstrate the ability of these methods to reproduce the experimental ΔG_{solv}. It is worth noting that semiempirical results are only slightly worse than the *ab initio* values. Accordingly, they are an excellent alternative to more complex and expensive techniques for the calculation of ΔG_{solv} in CCl_4 solution.

Inspection of the *ab initio* and semiempirical van der Waals parameters (Table IV) reveals a high similarity. Thus, the averaged parameters for the three semiempirical methods ($C = 0.1082 \pm$

FIGURE 2. Comparison between 6-31G* and experimental estimates of the free energy of solvation.

TABLE V.
Semiempirical SCRF and Experimental Free Energies of Solvation (kcal / mol) in CCl$_4$.

Molecule	ΔG_{AM1}	ΔG_{MNDO}	ΔG_{PM3}	ΔG_{exp}
Phenol	−5.8	−5.7	−5.7	−6.1
Methanol	−2.5	−2.4	−2.5	−2.2
Acetic acid	−4.3	−4.2	−4.2	−3.4
Methyl acetate	−4.7	−4.6	−4.6	−3.7
Pyridine	−4.9	−4.9	−5.0	−5.0
Acetone	−4.0	−3.9	−4.1	−3.5
Ethanol	−3.0	−2.9	−2.9	−3.1
n-Propanol	−3.5	−3.5	−3.5	−3.7
n-Butanol	−4.1	−4.1	−4.1	−4.2
n-Pentanol	−4.7	−4.7	−4.7	−5.0
n-Hexanol	−5.3	−5.3	−5.3	−5.7
n-Heptanol	−5.9	−6.0	−5.9	−6.5
Propionic acid	−4.6	−4.6	−4.5	−4.3
Butyric acid	−5.2	−5.2	−5.1	−5.0
Ethylacetate	−5.2	−5.2	−5.1	−4.4
p-Hydroxy-benzaldehyde	−7.7	−7.7	−7.6	−8.2
p-Nitrophenol	−8.5	−8.6	−8.7	−9.4
m-Nitrophenol	−8.5	−8.6	−8.7	−8.8
p-Methylphenol	−6.4	−6.3	−6.2	−6.1
o-Methylphenol	−6.2	−6.1	−6.1	−6.8
Acetophenone	−7.1	−7.1	−7.1	−6.4
Aniline	−5.7	−5.6	−5.7	−5.7
Ethylamine	−3.0	−3.0	−3.0	−2.8
n-Propylamine	−3.5	−3.6	−3.6	−3.6
n-Butylamine	−4.1	−4.2	−4.2	−4.2
Trimethylamine	−3.2	−3.2	−3.3	−3.1
Diethylamine	−3.9	−4.0	−4.1	−4.1

0.0005, N = −0.0908 ± 0.0005, O = −0.0943 ± 0.0010, H = −0.0784 ± 0.0002) are very close to the 6-31G*-optimized values (C = 0.1080, N = −0.0901, O = −0.0929, H = −0.0771). This demonstrates the large transferability[8,9] of van der
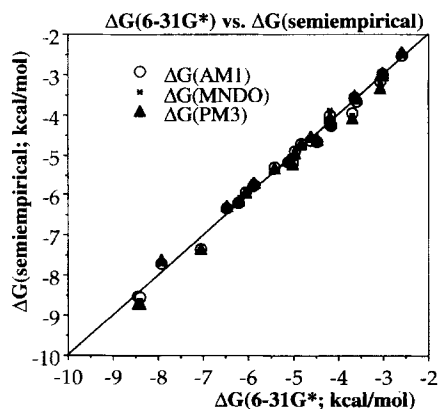

FIGURE 4. Comparison between 6-31G* and semiempirical estimates of the free energy of solvation.
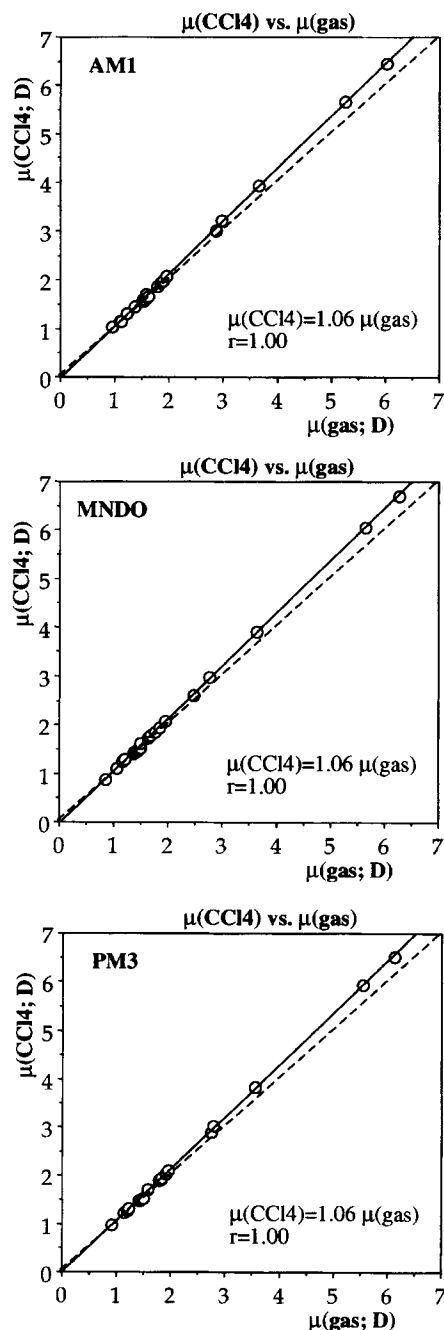

FIGURE 5. Comparison between semiempirical dipoles in gas phase and in CCl$_4$ solution. The dashed line corresponds to the ideal regression equation.

Waals parameters even for a solvent such as CCl$_4$, where van der Waals interactions play a key role in modulating the total free energy of solvation. Actually, the use of 6-31G*-optimized van der Waals parameters in semiempirical MST calculations provides very good results, as noted in Figure 6.
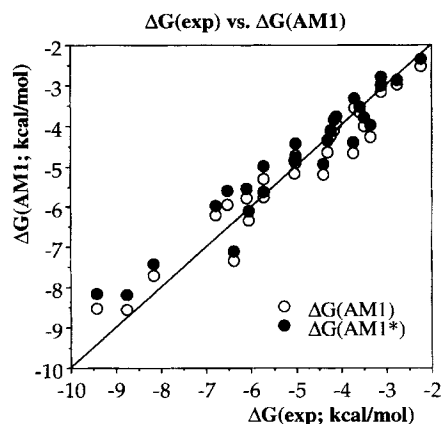
ΔG(exp) vs. ΔG(AM1)

○ ΔG(AM1)
● ΔG(AM1*)

FIGURE 6. Comparison between AM1 and experimental free energies of solvation. AM1, calculations performed with AM1-optimized van der Waals parameters. AM1*, calculations performed with 6-31G*-optimized van der Waals parameters.

TEST CALCULATIONS

The ultimate goal in the parametrization of the MST model is the study of chemical reactivity in a nonaqueous solvent, and particularly in CCl_4 solutions. To test the reliability of the optimized methods, test calculations were performed to study some prototypical chemical processes in CCl_4 solution.

Solvent Effect on Barrier to Amide Isomerization of Dimethylformamide

The description of solvent effects on amide isomerization, a process with marked solvent dependence and great biological implications, is a rele-

vant test for any theoretical model. Particularly, it is very delicate for SCRF methods, which are well suited for equilibrium solvent effects. Accordingly, they would tend to overestimate the solvent effect for transition states. The isomerization of small amides, like formamide, N-methylacetamide (NMA), dimethylformamide (DMF), and dimethylacetamide (DMA), has been studied in gas phase and aqueous solution using a wide variety of computational techniques.[26c, 38] Indeed, theoretical studies of the effect of nonaqueous solvent have also been reported.[39]

We analyzed the solvent effect on the isomerization of DMF, which has been used as a reduced model of proline.[40] Geometries for planar (GS) and twisted transition states (TS*syn* and *anti*, Fig. 7) were optimized at both *ab initio* 6-31G* and semiempirical levels. Frequency analysis was performed to verify the nature of minimum energy or the transition state of the optimized conformers. The gas-phase geometries were fixed in the computation of the ΔG_{solv} either in aqueous or CCl_4 solutions. Table VI shows the magnitude of the solvent effect, as determined from the difference in ΔG_{solv} between twisted and planar conformers $[\Delta\Delta G^{\neq} = \Delta G_{solv}(TS) - \Delta G_{solv}(GS)]$. For comparative purposes, theoretical values estimated from AM1(MC–QM/ MM) and OPLS(MC) calculations are also displayed.[39]

Data in Table VI stress the similarity between *ab initio* and semiempirical MST results in aqueous and CCl_4 solutions. The only noticeable discrepancy is the PM3 estimate of the solvent effect for the TS*syn*, which was not unexpected according to
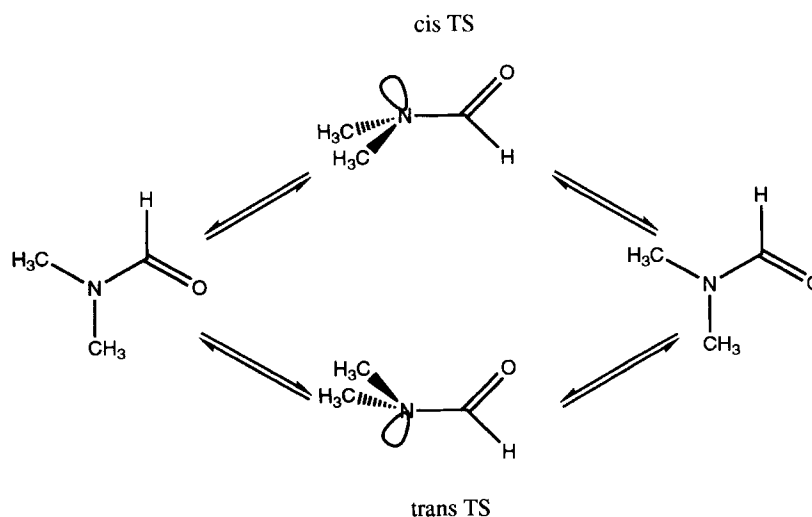
cis TS

trans TS

FIGURE 7. Scheme of the isomerization mechanism of dimethylformamide.

TABLE VI. _____
Solvent Effect on Activation Free Energy (kcal / mol) for Isomerization of Dimethylformamide.

Method	Solvent	TSanti	TSsyn
AM1 (MST)	H_2O	1.9	0.3
	CCl_4	0.7	0.2
MNDO (MST)	H_2O	1.5	0.0
	CCl_4	0.5	0.2
PM3 (MST)	H_2O	2.0	-0.4
	CCl_4	0.6	0.0
6-31G* (MST)	H_2O	2.8	1.0
	CCl_4	0.8	0.2
AM1 (MC-QM / MM)[a]	H_2O	2.7	0.5
	CCl_4	0.4	0.1
OPLS (MC)[b]	H_2O	2.8	-1.8
	CCl_4	0.4	0.1

[a] Ref. 39b.
[b] Data for dimethylacetamide.[39a]

previous studies.[9b] It is worth noting the close agreement between *ab initio* and semiempirical results for CCl_4 solutions, as well as with the available experimental data for amides. Thus, a water-induced destabilization of the TSanti up to 2.8 kcal/mol (6-31G*/MST) is found, which compares well with the experimental data for related amides[40] (for DMA a barrier increase of 4 kcal/mol is detected[‡]). The effect of changing from CCl_4 to aqueous solution (2 kcal/mol at the 6-31G*/MST level for the TSanti) also agrees with the experimental evidence (around 2 kcal/mol). The change in the activation free energy upon transfer from gas phase to CCl_4 is around 0.8 kcal/mol, which is slightly smaller than the experimental value of 1.5 kcal/mol. This latter discrepancy, which is systematically found for all the theoretical methods, could be partially due to amide aggregation.

The MST results are in reasonable agreement with results determined by Gao from MC–QM/MM calculations using OPLS parameters for water and CCl_4, and the AM1 Hamiltonian for DMF.[39b] The agreement with the values reported by Jorgensen and coworkers[39a] for DMA using classical MC simulations is also noticeable, especially regarding the effect of CCl_4. Thus, the solvent changes the TSanti and TSsyn barriers by 0.5–0.8 and 0.0–0.2 kcal/mol (0.4 and 0.1 kcal/mol according to MC–QM/MM and MC calculations).

[‡] It is known[27b, 40a] that the TSanti is preferred for DMA (and NMA) in both gas phase and aqueous solution.

The disagreement between MST and MC–QM/MM results from Jorgensen's MC values regarding the effect of water on the GS → TSsyn barrier merits some attention. Thus, Jorgensen and coworkers suggested a water-induced stabilization for the TSsyn of DMA of almost −2 kcal/mol, but for DMF our best estimate indicates a destabilization of +1 kcal/mol (+0.3 kcal/mol at the AM1/MST level). Gao's[34] AM1(MC–QM/MM) calculations give a destabilization of +0.5 kcal/mol. The reason for this disagreement is not clear. It appears to stem from the specific hydration characteristics of the TSsyn of DMF rather than from the intrinsic differences between the SCRF, MC–QM/MM, and classical MC calculations. This is supported by our previous findings for two related molecules, NMA and formamide,[9b, 26b] for which MST calculations indicated a stabilization of the TSsyn, in agreement with Jorgensen's results. Further investigation will be needed to clarify this point.

Solvent Effect on Tautomerism of 2-Pyridone

2-Pyridone has been widely studied as a model of the keto-amino ↔ enol-imino tautomerism of nucleic acids.[9b, 41] The large influence of the solvent on the tautomeric equilibrium is well known, and accordingly this system is a classical test. The performance of the MST methods to represent hydration effects on this tautomerism has been discussed in detail elsewhere.[9b, 42]

Table VII shows the changes in the keto ↔ enol tautomerization free energy (relative to the keto form) in CCl_4 of the cis (H cis to the N) and trans enol forms. The CCl_4 solvent effect on the keto-enol equilibrium is remarkable, especially when the most stable enol (cis) tautomer is considered. Thus, *ab initio* MST results indicate a large destabiliza-

TABLE VII. _____
Changes in Keto ↔ Enol Tautomerization Free Energy (kcal / mol) upon Transfer of 2-Pyridone from Gas Phase to CCl_4 Solution.

Method	ENOL(cis)[a]	ENOL(trans)[a]
AM1	+0.9	+0.2
MNDO	+0.7	+0.1
PM3	+0.9	+0.3
6-31G*	+1.2	+0.3
Experimental[b]	> 0.5	

[a] Cis, H(O) cis to N; trans, H(O) trans to N.
[b] Ref. 43.

tion of the enol tautomer in CCl_4 solution (around 1.2 kcal/mol). The semiempirical methods yield similar results, even though the magnitude of the solvent effect is slightly reduced. These results agree with the experimental data, which points out the enol form to be preferred in the gas phase, while the keto is the preferred form in CCl_4 solution.[43]

A Priori Calculation of Water / CCl_4 Transfer Free Energies

The quality of the MST values of ΔG_{solv} in aqueous and CCl_4 solutions enables the estimation, a priori, of partition coefficients and absolute free energies of transfer. Obviously, this is more susceptible to error than the calculation of ΔG_{solv} owing to error propagation. Assuming a quadratic propagation of the random error and that the rms deviation (rms in aqueous solution, 0.75 kcal/mol; rms in CCl_4 solution, 0.4 kcal/mol) is a good measure of the error, the uncertainty in transfer free energies between aqueous and CCl_4 solutions is estimated to be around 1.0 kcal/mol, even though larger errors might be found for some molecules. Considering the molecules (methanol, acetic acid, acetone, methylacetate, phenol, and pyridine) for which ab initio MST ΔG_{solv} values are available, the error with respect to the experimental data of the 6-31G*/MST transfer free energies ($\Delta G_{H_2O \rightarrow CCl_4}$) is precisely 1.0 kcal/mol. The transfer free energy has the incorrect sign only for phenol, which is due to the mediocre estimate of the hydration free energy.[9a]

Finally, the ΔG_{solv} in water and CCl_4 of three molecules not originally included in the series (p-aminobenzoic acid, benzamide, and o-nitrophenol) were also calculated. Results (see Table VIII) evidence the goodness of the method, which in all the cases yields estimates of log P within the expected range of error.

In summary, the MST-optimized methods have provided excellent estimates of the aqueous and CCl_4 solvent effect in a conformational change, i.e., the breaking of the peptide bond during the isomerization of amides. They have also captured the CCl_4-induced shift in the tautomeric preference of 2-hydroxypyridone. Finally, despite their intrinsic errors and the uncertainties due to error propagation, they seem able to estimate absolute partition coefficients with reasonable accuracy. These encouraging results open the possibility to rationalize and predict the solubility of molecules whose size precludes the use of other kinds of

TABLE VIII.
MST Solvation Free Energies (kcal / mol) in H_2O and CCl_4 and Partition Coefficient, log P (CCl_4 / H_2O).

	$\Delta G(H_2O)$	$\Delta G(CCl_4)$	log P
p-Aminobenzoic acid			
AM1	-11.4	-8.5	-2.2
MNDO	-11.6	-8.4	-2.3
PM3	-10.4	-8.3	-1.6
6-31G*	-10.8	-8.5	-1.7
Experimental[a]			-2.5
Benzamide			
AM1	-9.8	-7.7	-1.5
MNDO	-9.1	-7.6	-1.1
PM3	-10.0	-7.7	-1.7
6-31G*	-9.9	-7.9	-1.5
Experimental[a]			-1.5
o-Nitrophenol			
AM1 (MST)	-4.9	-7.6	2.0
MNDO (MST)	-6.9	-7.9	0.7
PM3 (MST)	-6.1	-7.7	1.2
6-31G* (MST)	-4.3	-7.3	2.2
Experimental[a]			1.9

[a] Ref. 25a.

calculation, like those based on double annihilation approaches within the Free Energy Perturbation framework.

Acknowledgments

References

1. (a) C. Reichart, Solvents and Solvent Effects in Organic Chemistry, VCH, New York, 1990; (b) W. Breslow, Acc. Chem. Res., 24, 159 (1991); (c) W. L. Jorgensen, Chemtracts Org. Chem., 4, 91 (1991).

2. L. Onsager, J. Am. Chem. Soc., 58, 1486 (1936).

3. (a) J. G. Kirkwood, *J. Chem. Phys.*, **2**, 351 (1934); (b) J. G. Kirkwood and F. H. Westheimer, *J. Chem. Phys.*, **6**, 506 (1938).

4. (a) J. L. Rivail and D. Rinaldi, *Theor. Chim. Acta*, **32**, 57 (1973); (b) O. Tapia and O. Goscinski, *Mol. Phys.*, **29**, 1653 (1975); (c) S. Miertus, E. Scrocco, and J. Tomasi, *Chem. Phys.*, **55**, 117 (1981); (d) M. M. Karelson, T. Tamm, A. R. Katritzky, S. J. Cato, and M. Zerner, *Tetrahedron Comput. Methodol.*, **2**, 295 (1989); (e) B. Wang and G. P. Ford, *J. Comput. Chem.*, **97**, 4162 (1992); (f) M. J. Negre, M. Orozco, and F. J. Luque, *Chem. Phys. Lett.*, **196**, 27 (1992); (g) G. E. Chudinov, D. V. Napolov, and M. U. Basilevsky, *Chem. Phys.*, **160**, 41 (1992); (h) C. J. Cramer and D. G. Truhlar, *Science*, **256**, 213 (1992); (i) V. Luzhkov and A. Warshel, *J. Comput. Chem.*, **13**, 199 (1993); (j) G. Rauhut, T. Clark, and T. Steinke, *J. Am. Chem. Soc.*, **115**, 9174 (1993).

5. (a) J. L. Pascual-Ahuir, E. Silla, J. Tomasi, and R. Bonaccorsi, *J. Comput. Chem.*, **8**, 778 (1987); (b) J. L. Pascual-Ahuir and E. Silla, *J. Am. Chem.*, **9**, 1047 (1990); (c) E. Silla, I. Tuñón, and J. L. Pascual-Ahuir, *J. Comput. Chem.*, **12**, 1077 (1991); (d) J. Tomasi, G. Alagona, R. Bonaccorsi, C. Ghio, and R. Cammi, In *Theoretical Model of Chemical Bonding*, Vol. 4, Z. Maksic, Ed., Springer-Verlag, Berlin, 1991; (e) J. Tomasi and M. Persico, *Chem. Rev.*, **94**, 2027 (1994).

6. (a) F. Floris and J. Tomasi, *J. Comput. Chem.*, **10**, 616 (1989); (b) F. M. Floris, J. Tomasi, and J. L. Pascual-Ahuir, *J. Comput. Chem.*, **12**, 784 (1991).

7. J. Tomasi, R. Bonaccorsi, R. Cammi, and F. J. Olivares del Valle, *J. Mol. Struct.: Theochem.*, **234**, 401 (1991); (b) F. J. Olivares del Valle and M. A. Aguilar, *J. Comput. Chem.*, **13**, 115 (1992); (c) F. J. Luque, M. J. Negre, and M. Orozco, *J. Phys. Chem.*, **97**, 4386 (1993).

8. (a) M. Bachs, F. J. Luque, and M. Orozco, *J. Comput. Chem.*, **15**, 446 (1994); (b) M. Orozco and F. J. Luque, *Chem. Phys.*, **182**, 237 (1994).

9. (a) F. J. Luque, M. Bachs, and M. Orozco, *J. Comput. Chem.*, **15**, 847 (1994); (b) M. Orozco, M. Bachs, and F. J. Luque, *J. Comput. Chem.*, **16**, 563 (1995).

10. (a) C. J. Cramer and D. G. Truhlar, *J. Comput.-Aided Mol. Design*, **6**, 629 (1992); (b) G. P. Ford and B. Wang, *J. Mol. Struct.: Theochem.*, **283**, 49 (1993); (c) M. Szafran, M. M. Karelson, A. R. Katritzky, J. Koput, and M. C. Zerner, *J. Comput. Chem.*, **14**, 371 (1993); (d) C. J. Cramer and D. G. Truhlar, *J. Am. Chem. Soc.*, **115**, 8810 (1993).

11. (a) R. Bonaccorsi, F. Floris, and J. Tomasi, *J. Mol. Liquids*, **47**, 25 (1990); (b) R. Bonaccorsi, E. Ojalvo, P. Palla, and J. Tomasi, *Chem. Phys.*, **143**, 245 (1990); (c) M. Cossi, M. Persico, and J. Tomasi, *J. Am. Chem. Soc.*, **116**, 5373 (1994).

12. D. J. Giesen, J. W. Storer, C. J. Cramer, and D. G. Truhlar, *J. Am. Chem. Soc.*, **117**, 1057 (1995).

13. P. C. Hariharan and J. A. Pople, *Theor. Chim. Acta*, **28**, 213 (1978).

14. M. J. S. Dewar, E. G. Zoebisch, E. F. Healy, and J. J. P. Stewart, *J. Am. Chem. Soc.*, **107**, 3902 (1985).

15. M. J. S. Dewar and W. Thiel, *J. Am. Chem. Soc.*, **99**, 4899 (1977).

16. J. J. P. Stewart, *J. Comput. Chem.*, **10**, 209 (1989).

17. C. J. Böttcher, *Theory of Electric Polarization*, Elsevier, Amsterdam, 1952, Chap. 5.

18. E. Scrocco and J. Tomasi, *Topics Curr. Chem.*, **42**, 95 (1973).

19. (a) G. G. Ferenczy, C. A. Reynolds, and W. G. Richards, *J. Comput. Chem.*, **11**, 159 (1990); (b) C. Alhambra, F. J. Luque, and M. Orozco, *J. Comput. Chem.*, **15**, 12 (1994).

20. (a) F. J. Luque, F. Illas, and M. Orozco, *J. Comput. Chem.*, **11**, 416 (1990); (b) B. H. Besler, K. M. Merz, and P. A. Kollman, *J. Comput. Chem.*, **11**, 909 (1990); (c) F. J. Luque, and M. Orozco, *Chem. Phys. Lett.*, **168**, 269 (1990); (d) C. Alemán, F. J. Luque, and M. Orozco, *J. Comput. Chem.*, **14**, 799 (1993).

21. (a) R. A. Pierotti, *Chem. Rev.*, **76**, 717 (1976); (b) O. Sinanoglu, *J. Chem. Phys.*, **75**, 463 (1981); (c) I. Tuñón, E. Silla, and J. L. Pascual-Ahuir, *Chem. Phys. Lett.*, **203**, 289 (1993); (d) V. Gogonea and E. Osawa, *J. Mol. Struct.: Theochem.*, **311**, 305 (1994).

22. (a) D. Eisenberg and A. D. McLachlan, *Nature*, **319**, 199 (1986); (b) F. Vigné-Maeder and P. Claverie, *J. Am. Chem. Soc.*, **109**, 24 (1987); (c) T. Ooi, M. Oobatake, G. Némethy, and H. A. Scheraga, *Proc. Natl. Acad. Sci. USA*, **84**, 3086 (1987).

23. I. Tuñón, E. Silla, and J. L. Pascual-Ahuir, *J. Phys. Chem.*, **98**, 377 (1994), and references therein.

24. D. R. Lide, Ed., *Handbook of Chemistry and Physics*, 74th eds., CRC Press, Boca Raton, FL, 1993–1994.

25. (a) M. G. Koehler, S. Grigoras, and W. J. Dunn III. *Quant. Struct.-Act. Relat.*, **7**, 150 (1988); (b) A. Ben-Naim and Y. Marcus, *J. Chem. Phys.*, **81**, 2106 (1984); (c) R. G. Pearson, *J. Am. Chem. Soc.*, **108**, 6109 (1986); (d) S. Cabani, P. Giani, V. Mollica and L. Lepori, *J. Solut. Chem.*, **10**, 563 (1981).

26. (a) M. Orozco, W. L. Jorgensen, and F. J. Luque, *J. Comput. Chem.*, **14**, 1498 (1993); (b) F. J. Luque and M. Orozco, *J. Org. Chem.*, **58**, 6397 (1993); (c) M. Orozco and F. J. Luque, *J. Am. Chem. Soc.*, **117**, 1378 (1995).

27. W. L. Jorgensen, BOSS, Version 3.4, Yale University, New Haven, CT, 1990.

28. W. L. Jorgensen, J. M. Briggs, and M. L. Contreras, *J. Phys. Chem.*, **94**, 1683 (1990).

29. (a) F. A. Momany, *J. Phys. Chem.*, **82**, 592 (1978); (b) S. R. Cox and D. E. Williams, *J. Comput. Chem.*, **2**, 304 (1981); (c) U. C. Singh and P. A. Kollman, *J. Comput. Chem.*, **5**, 129 (1984); (d) R. Bonaccorsi, E. Scrocco, C. Petrongolo, and J. Tomasi, *Theor. Chim. Acta*, **20**, 331 (1984); (e) M. Orozco and F. J. Luque, *J. Comput. Chem.*, **11**, 909 (1990).

30. M. A. Aguilar, F. J. Olivares del Valle, and J. Tomasi, *J. Chem. Phys.*, **98**, 7375 (1993).

31. M. J. Frisch, G. W. Trucks, M. Head-Gordon, P. M. W. Gill, M. W. Wong, J. B. Foresman, B. G. Johnson, H. B. Schlegel, M. A. Robb, E. S. Replogle, R. Gomperts, J. L. Andres, K. Raghavachari, J. S. Binkley, C. Gonzalez, R. L. Martin, D. J. Fox, D. J. Defrees, J. Baker, J. J. P. Stewart, and J. A. Pople, Gaussian 92, Gaussian Inc., Pittsburgh, PA, 1992.

32. M. Peterson and R. Poirier, MONSTERGAUSS, Dept. of Biochemistry, Univ. of Toronto, Canada, version modified by R. Cammi, R. Bonaccorsi, and J. Tomasi, 1987.

33. J. J. P. Stewart, MOPAC-93 Rev 2, Fujitsu Limited, 1993.

34. J. Gao, personal communication.

35. N. S. Bayliss and E. G. McRae, *J. Phys. Chem.*, **58**, 1006 (1954).

36. (a) R. Bonaccorsi, R. Cimiraglia, and J. Tomasi, *J. Comput. Chem.*, **4**, 567 (1983); (b) R. Bonaccorsi, R. Cimiraglia, and J. Tomasi, *J. Mol. Struct.: Theochem.*, **107**, 197 (1984); (c) M. Karelson and M. C. Zerner, *J. Am. Chem. Soc.*, **112**, 9405 (1990); (d) T. Fox and N. Rösch, *Chem. Phys. Lett.*, **191**, 33 (1992); (e) T. Fox and N. Rösch, *J. Mol. Struct.: Theochem.*, **276**, 279 (1992).

37. (a) S. E. DeBolt and P. A. Kollman, *J. Am. Chem. Soc.*, **112**, 7515 (1990); (b) J. Gao, *J. Am. Chem. Soc.*, **116**, 9324 (1994).

38. (a) W. L. Jorgensen and J. Gao, *J. Am. Chem. Soc.*, **110**, 4212 (1989); (b) G. Alagona, C. Ghio, J. Igual, and J. Tomasi, *J. Mol. Struct.: Theochem.*, **204**, 253 (1990); (c) P. Cieplak and P. Kollman, *J. Comput. Chem.*, **12**, 1232 (1991); (d) S. Tsuzuki and K. Tanabe, *J. Chem. Soc., Perkin Trans. 2*, 1255 (1991); (e) K. B. Wiberg and C. M. Breneman, *J. Am. Chem. Soc.*, **114**, 831 (1992); (f) J. Gao, *J. Am. Chem. Soc.*, **115**, 2930 (1993).

39. (a) E. M. Duffy, D. L. Severance, and W. L. Jorgensen, *J. Am. Chem. Soc.*, **114**, 7535 (1992); (b) J. Gao, *Proc. Ind. Acad. Sci., Chem. Sci.*, **106**, 507 (1994).

40. (a) T. Drakenberg, K. I. Dahlqvist, and S. Forsen, *J. Phys. Chem.*, **76**, 2178 (1972); (b) M. Feigel, *J. Phys. Chem.*, **87**, 3054

(1983); (c) B. D. Ross and N. S. True, *J. Am. Chem. Soc.*, **106**, 2451 (1984).

41. (a) P. Cieplak, P. Bash, U. C. Singh, and P. A. Kollman, *J. Am. Chem. Soc.*, **109**, 6283 (1987); (b) C. J. Cramer and D. G. Truhlar, *J. Am. Chem. Soc.*, **113**, 8552 (1991); (c) M. Szafran, M. M. Karelson, A. R. Katritzky, J. Koput, and M. C. Zerner, *J. Comput. Chem.*, **14**, 371 (1993); (d) J. Gao and L. Shao, *J. Phys. Chem.*, to appear.

42. C. Alhambra, F. J. Luque, J. Estelrich, and M. Orozco, *J. Org. Chem.*, **60**, 969 (1995).

42. (a) S. F. Mason, *J. Chem. Soc.*, 4874 (1957); (b) P. Beak, F. S. Fry, J. Lee, and F. Steele, *J. Am. Chem. Soc.*, **98**, 8284 (1976).